ISSN 1948-5204 (online)

World Journal of *Gastrointestinal Oncology*

World J Gastrointest Oncol 2024 April 15; 16(4): 1091-1675

Published by Baishideng Publishing Group Inc

World Journal of Gastrointestinal Oncology

Contents

Monthly Volume 16 Number 4 April 15, 2024

World Journal of Gastrointestinal Oncology

Monthly Volume 16 Number 4 April 15, 2024

Contents

World Journal of Gastrointestinal Oncology

Monthly Volume 16 Number 4 April 15, 2024

Contents

ABOUT COVER

Peer Reviewer of *World Journal of Gastrointestinal Oncology*, Lie Zheng, Director, Professor, Department of Gastroenterology, Shaanxi Provincial Hospital of Traditional Chinese Medicine, Xi'an 730000, Shaanxi Province, China. xinliwen696@126.com

AIMS AND SCOPE

The primary aim of *World Journal of Gastrointestinal Oncology* (*WJGO*, *World J Gastrointest Oncol*) is to provide scholars and readers from various fields of gastrointestinal oncology with a platform to publish high-quality basic and clinical research articles and communicate their research findings online.

WJGO mainly publishes articles reporting research results and findings obtained in the field of gastrointestinal oncology and covering a wide range of topics including liver cell adenoma, gastric neoplasms, appendiceal neoplasms, biliary tract neoplasms, hepatocellular carcinoma, pancreatic carcinoma, cecal neoplasms, colonic neoplasms, colorectal neoplasms, duodenal neoplasms, esophageal neoplasms, gallbladder neoplasms, *etc*.

INDEXING/ABSTRACTING

The *WJGO* is now abstracted and indexed in PubMed, PubMed Central, Science Citation Index Expanded (SCIE, also known as SciSearch®), Journal Citation Reports/Science Edition, Scopus, Reference Citation Analysis, China Science and Technology Journal Database, and Superstar Journals Database. The 2023 edition of Journal Citation Reports® cites the 2022 impact factor (IF) for *WJGO* as 3.0; IF without journal self cites: 2.9; 5-year IF: 3.0; Journal Citation Indicator: 0.49; Ranking: 157 among 241 journals in oncology; Quartile category: Q3; Ranking: 58 among 93 journals in gastroenterology and hepatology; and Quartile category: Q3. The *WJGO*'s CiteScore for 2022 is 4.1 and Scopus CiteScore rank 2022: Gastroenterology is 71/149; Oncology is 197/366.

RESPONSIBLE EDITORS FOR THIS ISSUE

Production Editor: *Xiang-Di Zhang*; **Production Department Director:** *Xiang Li*; **Cover Editor:** *Jia-Ru Fan*.

NAME OF JOURNAL
World Journal of Gastrointestinal Oncology

ISSN
ISSN 1948-5204 (online)

LAUNCH DATE
February 15, 2009

FREQUENCY
Monthly

EDITORS-IN-CHIEF
Monjur Ahmed, Florin Burada

EDITORIAL BOARD MEMBERS
https://www.wjgnet.com/1948-5204/editorialboard.htm

PUBLICATION DATE
April 15, 2024

INSTRUCTIONS TO AUTHORS
https://www.wjgnet.com/bpg/gerinfo/204

GUIDELINES FOR ETHICS DOCUMENTS
https://www.wjgnet.com/bpg/GerInfo/287

GUIDELINES FOR NON-NATIVE SPEAKERS OF ENGLISH
https://www.wjgnet.com/bpg/gerinfo/240

PUBLICATION ETHICS
https://www.wjgnet.com/bpg/GerInfo/288

PUBLICATION MISCONDUCT
https://www.wjgnet.com/bpg/gerinfo/208

ARTICLE PROCESSING CHARGE
https://www.wjgnet.com/bpg/gerinfo/242

STEPS FOR SUBMITTING MANUSCRIPTS
https://www.wjgnet.com/bpg/GerInfo/239

ONLINE SUBMISSION
https://www.f6publishing.com

World Journal of Gastrointestinal Oncology

Submit a Manuscript: https://www.f6publishing.com

World J Gastrointest Oncol 2024 April 15; 16(4): 1296-1308

DOI: 10.4251/wjgo.v16.i4.1296

ISSN 1948-5204 (online)

ORIGINAL ARTICLE

Observational Study

Computed tomography radiogenomics: A potential tool for prediction of molecular subtypes in gastric stromal tumor

Xiao-Nan Yin, Zi-Hao Wang, Li Zou, Cai-Wei Yang, Chao-Yong Shen, Bai-Ke Liu, Yuan Yin, Xi-Jiao Liu, Bo Zhang

Specialty type: Gastroenterology & hepatology

Provenance and peer review: Unsolicited article; Externally peer reviewed.

Peer-review model: Single blind

Peer-review report's scientific quality classification

Grade A (Excellent): 0
Grade B (Very good): 0
Grade C (Good): C
Grade D (Fair): 0
Grade E (Poor): 0

P-Reviewer: Dimofte GM, Romania

Received: October 8, 2023
Peer-review started: October 8, 2023
First decision: January 15, 2024
Revised: January 23, 2024
Accepted: February 25, 2024
Article in press: February 25, 2024
Published online: April 15, 2024

Xiao-Nan Yin, Zi-Hao Wang, Chao-Yong Shen, Bai-Ke Liu, Yuan Yin, Gastric Cancer Research Center, West China Hospital, Sichuan University, Chengdu 610041, Sichuan Province, China

Li Zou, Department of Paediatric Surgery, West China Hospital of Sichuan University, Chengdu 610041, Sichuan Province, China

Cai-Wei Yang, Xi-Jiao Liu, Department of Radiology, West China Hospital, Sichuan University, Chengdu 610041, Sichuan Province, China

Bo Zhang, Department of Gastrointestinal Surgery, Sichuan University West China Hospital, Chengdu 610041, Sichuan Province, China

Corresponding author: Xi-Jiao Liu, PhD, Doctor, Department of Radiology, West China Hospital, Sichuan University, No. 37 Guoxue Lane, Wuhou District, Chengdu 610041, Sichuan Province, China. bless_jiao@163.com

Abstract

BACKGROUND

Preoperative knowledge of mutational status of gastrointestinal stromal tumors (GISTs) is essential to guide the individualized precision therapy.

AIM

To develop a combined model that integrates clinical and contrast-enhanced computed tomography (CE-CT) features to predict gastric GISTs with specific genetic mutations, namely *KIT* exon 11 mutations or *KIT* exon 11 codons 557-558 deletions.

METHODS

A total of 231 GIST patients with definitive genetic phenotypes were divided into a training dataset and a validation dataset in a 7:3 ratio. The models were constructed using selected clinical features, conventional CT features, and radiomics features extracted from abdominal CE-CT images. Three models were developed: $Model_{CT\ sign}$, $model_{CT\ sign + rad}$, and model $CT_{sign + rad + clinic}$. The diagnostic performance of these models was evaluated using receiver operating characteristic (ROC) curve analysis and the Delong test.

RESULTS

The ROC analyses revealed that in the training cohort, the area under the curve (AUC) values for $model_{CT\ sign}$, $model_{CT\ sign + rad}$, and $model_{CT\ sign + rad + clinic}$ for predicting *KIT* exon 11 mutation were 0.743, 0.818, and 0.915, respectively. In the validation cohort, the AUC values for the same models were 0.670, 0.781, and 0.811, respectively. For predicting *KIT* exon 11 codons 557-558 deletions, the AUC values in the training cohort were 0.667, 0.842, and 0.720 for $model_{CT\ sign}$, $model_{CT\ sign + rad}$, and $model_{CT\ sign + rad + clinic}$, respectively. In the validation cohort, the AUC values for the same models were 0.610, 0.782, and 0.795, respectively. Based on the decision curve analysis, it was determined that the $model_{CT\ sign + rad + clinic}$ had clinical significance and utility.

CONCLUSION

Our findings demonstrate that the combined $model_{CT\ sign + rad + clinic}$ effectively distinguishes GISTs with *KIT* exon 11 mutation and *KIT* exon 11 codons 557-558 deletions. This combined model has the potential to be valuable in assessing the genotype of GISTs.

Key Words: Gastrointestinal stromal tumor; Radiomics; Gene mutation; Computed tomography; Model

Core Tip: In this study, we developed and validated a radiomics model to predict the genotypes of gastric gastrointestinal stromal tumors (GISTs) using contrast-enhanced computed tomography images. Our findings demonstrated that the radiomics model exhibited a satisfactory performance in distinguishing gastric GISTs with *KIT* exon 11 mutations and GISTs with *KIT* exon 11 codons 557-558 deletions. Among the different models evaluated, the combined $model_{CT\ sign + rad + clinic}$ demonstrated the highest predictive accuracy. This model holds promise as an effective and noninvasive approach to guide personalized treatment decisions prior to surgery.

Citation: Yin XN, Wang ZH, Zou L, Yang CW, Shen CY, Liu BK, Yin Y, Liu XJ, Zhang B. Computed tomography radiogenomics: A potential tool for prediction of molecular subtypes in gastric stromal tumor. *World J Gastrointest Oncol* 2024; 16(4): 1296-1308
URL: https://www.wjgnet.com/1948-5204/full/v16/i4/1296.htm
DOI: https://dx.doi.org/10.4251/wjgo.v16.i4.1296

INTRODUCTION

Gastrointestinal stromal tumor (GIST) is the most common mesenchymal tumor of the gastrointestinal tract, with an annual incidence ranging from 6 to 22 cases per million individuals[1,2]. The stomach is the primary site of GIST onset, accounting for 60%-65% of cases[3]. Prior to the year 2000, advanced GISTs had no effective medical therapy due to their poor response to chemotherapy and radiotherapy. However, the identification of activating *KIT* mutations in GISTs led to the rapid development of the first tyrosine kinase inhibitor (TKI), imatinib, which significantly improved clinical outcomes for GIST patients[4,5]. In addition to *KIT* mutations, mutations in other genes such as *PDGFRA*, NF-1, BRAF, KRAS, and PIK3CA, as well as SDH deficiency, have been discovered in GISTs[1,6]. The presence of specific driver oncogenic genes in GISTs has made it a paradigm for precision medicine treatment.

The majority of GISTs harbor *KIT* mutations (80%) or *PDGFRA* mutations (5%-10%)[7,8]. Testing for *KIT* and *PDGFRA* mutations is crucial for defining GIST pathological diagnosis, predicting tumor prognosis, and guiding TKI therapy. Studies have shown that patients with *PDGFRA* mutations have a better prognosis compared to those with *KIT* mutations [9]. Among GIST patients with *KIT* exon 11 mutations, those with deletion or insertion-deletion mutations have a worse prognosis than those with point or repeat mutations. In addition, the presence of multiple codon deletion mutations or deletions affecting codons 557-558 on *KIT* exon 11 has been linked to an aggressive biological phenotype and an unfavorable prognosis[10,11]. It has been clinically observed that GISTs exhibit different response rates to imatinib depending on their mutation status. GISTs with *KIT* exon 11 mutations have a higher response rate and recurrence-free survival to standard imatinib therapy compared to exon 9 tumors. Most *PDGFRA* mutations respond to imatinib, with the exception of D842V. Therefore, predicting the mutation status of tumors is crucial for managing GISTs. However, currently, tumor mutation status can only be obtained after surgical resection or conventional invasive biopsy, making preoperative genotyping of GISTs more challenging.

Contrast-enhanced computed tomography (CE-CT) is routinely used in clinical practice for the detection and evaluation of GISTs. Recent advancements in CT image acquisition have enabled the acquisition of high-quality isotropic images that provide rich data beyond general morphological information. Radiomics, an emerging quantitative imaging method, can convert high-throughput medical imaging features into quantitative data. It has been extensively applied for differential diagnosis, prognostic prediction, prediction of biological behavior, treatment outcomes, and tumor genetics [12-15]. Previous studies have demonstrated that radiomics features can predict the malignant potential and prognosis of GIST[16-19]. Radiogenomics, a promising paradigm, integrates clinical imaging with molecular and genomic imaging. However, there have been limited studies on radiomics for predicting the mutational status of GISTs[20-22].

In 2021, the primary outcomes of our research were published[21]. The study revealed associations between GISTs with *KIT* exon 11 mutations and CE-CT images. CT radiogenomics showed promising potential in predicting the *KIT* exon 11 mutation status of GISTs. This study focuses specifically on gastric GISTs and aims to develop a prediction model for genotypes using CE-CT images.

MATERIALS AND METHODS

Patients

This retrospective study obtained ethical approval from the Research Ethics Board of West China Hospital, Sichuan University, China [Number: 2022(449)], and informed consent was waived due to the nature of the study. The inclusion criteria were as follows: (1) Patients who underwent CE-CT examination at our hospital within 30 d prior to surgery or biopsy; (2) patients diagnosed with primary gastric GISTs confirmed by pathological examination; and (3) patients with definitive genetic analysis results. The exclusion criteria were as follows: (1) Patients who received preoperative antitumoral treatment; (2) patients with tumor rupture; and (3) patients with inadequate CE-CT image quality, such as severe motion artifact or portal phase image thickness exceeding 5 mm. A total of 231 patients from May 2010 to December 2021 were included in the study (Figure 1). Mutation analysis was performed on the coding sequence of the *KIT* gene (exon 9, 11, 13, and 17) and the *PDGFRA* gene (exon 12, 14, and 18) using Sanger sequencing. Clinical information and pathology results were also collected.

CT imaging acquisition

All CT examinations were performed using three different CT scanners: A 64-slice CT scanner (Philips Medical system, Eindhoven, The Netherlands), a 128-slice CT scanner (SOMATOM Definition AS +, Siemens Healthcare, Germany), and a dual-source CT system (Somatom Definition Flash, Siemens Healthcare, Germany). Prior to the CT examination, patients were required to fast for at least 6 h and ingest 600-1000 mL of water. The CT scanning range encompassed the entire abdomen. The parameters for the CT examinations were as follows: Tube voltage of 120 kV, tube current ranging from 145 to 200 mAs, slice thickness of 2-5 mm, slice interval of 2 mm, field of view ranging from 35 cm to 50 cm, matrix size of 512 × 512, rotation time of 0.5 s, and pitch of 1.0. In all patients, an iodinated contrast agent (1.2-1.5 mL/kg) was intravenously injected using a syringe pump. Enhanced images were acquired during the arterial phase triggered at a threshold of 170 hounsfield units, and the portal venous phase was captured 30 s after the trigger.

CT imaging analysis

The CT images were independently reviewed by two radiologists who were blinded to the clinicopathological data. Discrepancies between the two radiologists were resolved through consensus. The following CT features were evaluated using Syngo Imaging Workplaces (VersionVB35A, Siemens AG, Erlangen, Germany): Tumor location, size, shape (regular or irregular), margin (well-defined or ill-defined), growth pattern (exophytic, endophytic, or mixed), density (hypodensity, isodensity, or hyperdensity), enhancement pattern and degree (mild, moderate, or marked), presence of internal low attenuation areas (necrosis, gas, or cystic degeneration), calcification, superficial ulceration, presence of intra-tumoral vessels, infiltration of adjacent mesangial fat, invasion of adjacent organs, distant metastasis, and lymphadenopathy. The CT attenuation value was measured by delineating the region of interest (ROI) along the tumor edge on each consecutive slice covering the entire lesion, excluding vessels, gas, and necrotic areas. Tumor necrosis was defined as an irregular area within the tumor with a CT attenuation value < 20 HU in each phase and an enhancement increase of less than 10 HU among the three phases. Cystic degeneration was characterized as a region with a smooth and well-defined border and a density similar to water (CT attenuation value of 0-20 HU).

Radiomic analysis

All CE-CT images were collected and exported to the ITK-SNAP software (version 3.6.0, http://www.itk-snap.org) for manual segmentation of the ROI. For each patient, the portal vein phase images were reviewed, and the two largest cross-section slices were selected. ROIs were delineated over the solid portion of the entire lesion, excluding gas, calcification, vessels, and necrotic areas. The segmentation procedure was independently performed by two radiologists.

The Intelligence Foundry (Version 1.2, General Electric) was utilized to extract radiomics features from the lesions. A total of 554 features, comprising Original features, Co-occurrence of Local Anisotropic Gradient Orientations features, and Wavelet and local binary pattern (Wavelet-LBP) features, were extracted using PyRadiomic[23]. The reproducibility of the features was evaluated by calculating intra- and inter-class correlation coefficients (ICCs). Radiomics features that exhibited ICC values exceeding 0.75 in both intra- and inter-observer comparisons were selected for further feature analysis.

The entire dataset was randomly divided into training and internal validation datasets in a 7:3 ratio. The training dataset was exclusively used for feature selection and modeling. The feature preprocessing, feature selection, and modeling methods were as follows.

Based on the features identified through the ICC analysis, features with a variance less than 1.0 were excluded. Outlier values greater than the third quartile plus twice the interquartile range were converted to the 95th percentile, while values less than the first quartile minus twice the interquartile range were converted to the 10th percentile. To address the class imbalance in the training dataset, the synthetic minority oversampling technique was employed, with 200% oversampling and 150% undersampling[24]. Subsequently, all features were normalized and standardized using the Z-Score method.

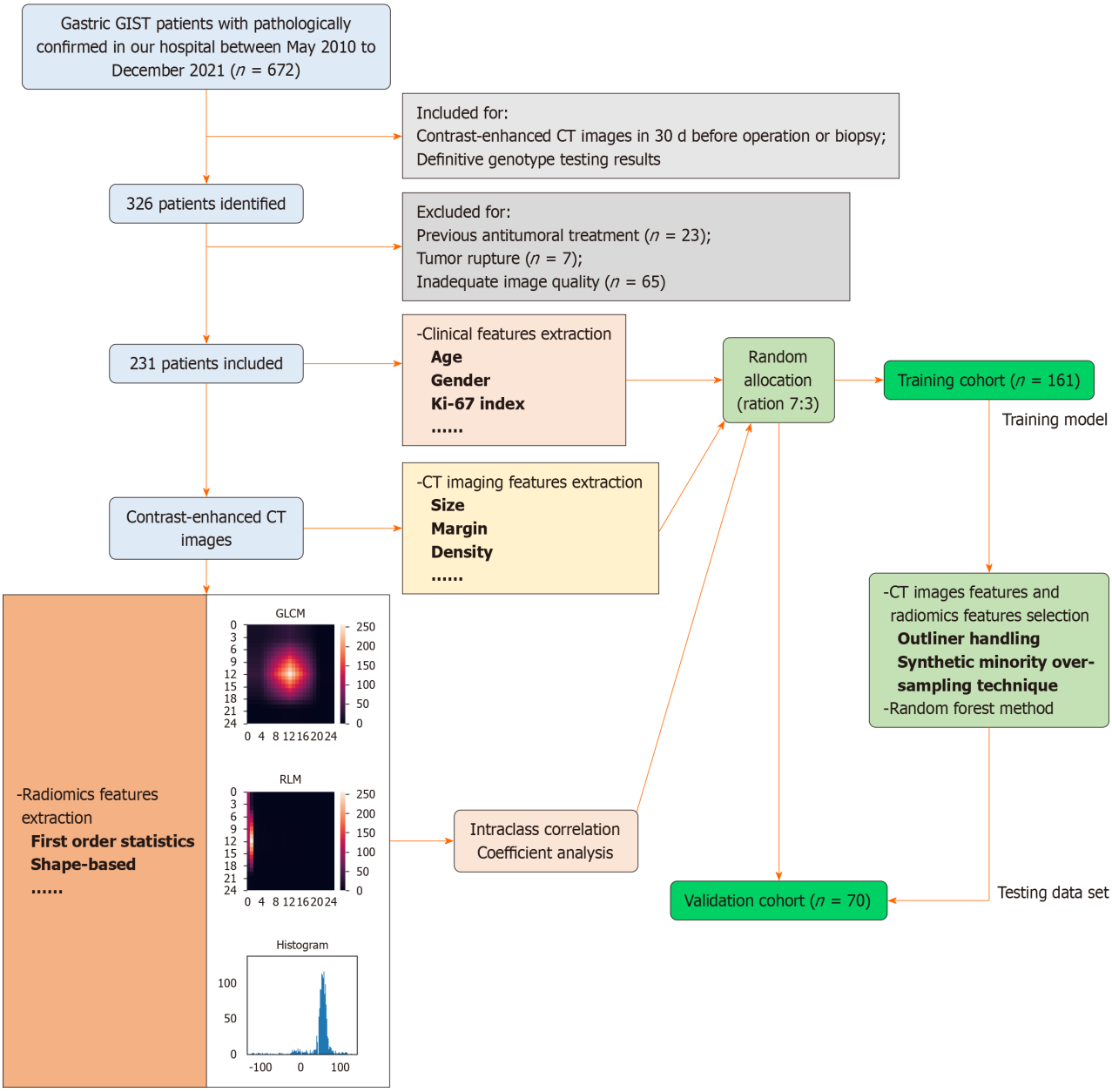

Figure 1 Study workflow. GIST: Gastrointestinal stromal tumor; CT: Computed tomography.

The feature importance was evaluated using random forest (RF) based on the mean decrease of Gini calculated for all decision trees in the RF model. The top three important features were selected and used to construct the RF model[25,26].

Statistical analysis

Statistical analysis was conducted using SPSS software (Version 19, Chicago, IL, United States) and R software (Version 3.6.3; http://www.Rproject.org). All statistical significance levels were two-sided, and a significance level of $P < 0.05$ was considered statistically significant. To compare the significant differences between different genotype groups in both the training and validation cohorts, the Mann-Whitney *U* test or independent sample *t*-test was employed. Fisher's exact test or chi-square test was utilized to identify significant differences between different groups of continuous variables. The discrimination performance of the models was evaluated using receiver operating characteristic (ROC) curves. The area under the ROC curve (AUC) was used as a comprehensive measure of performance. Specificity, sensitivity, and positive and negative predictive values were used to assess model performance at specific thresholds, which were determined by maximizing the Youden index. The Delong test was employed to compare the AUC of paired models. Internal validation was estimated by performing regular bootstrapping with 1000 bootstrap samples[27]. The goodness-of-fit of the model was assessed using the Hosmer-Lemeshow test, with a *P*-value greater than 0.05 indicating agreement between the observed and predicted values. Model calibration was visualized using calibration curve analysis, and the clinical net benefit of the model was evaluated using decision curve analysis (DCA).

Table 1 Clinicopathological characteristics of gastrointestinal stromal tumor patients included in this study, *n* (%)

Characteristics	*KIT* exon 11 mutation (*n* = 192)	Without *KIT* exon 11 mutation (*n* = 39)	*P* value	*KIT* exon 11 mutation with deletions involving codons 557-558 (*n* = 56)	*KIT* exon 11 mutation without deletions involving codons 557-558 (*n* = 136)	*P* value
Gender (male)	97 (50.5)	24 (61.5)	0.223	32 (57.1)	65 (47.8)	0.268
Age	55.7 ± 11.5	53.8 ± 13.4	0.360	53.9 ± 13.5	56.4 ± 10.6	0.222
Mitosis						
≤ 5/50 HPF	91 (47.4)	24 (61.5)	0.117	11 (19.6)	80 (58.8)	< 0.010
> 5/50 HPF	101 (52.6)	15 (38.5)		45 (80.4)	56 (41.2)	
Risk classification						
Very low	2 (1.0)	0 (0)	0.851	0 (0)	2 (1.5)	< 0.010
Low	43 (22.4)	10 (25.7)		4 (7.1)	39 (28.7)	
Intermediate	59 (30.8)	13 (33.3)		7 (12.5)	52 (38.2)	
High	88 (45.8)	16 (41.0)		45 (80.4)	43 (31.6)	

RESULTS

Clinicopathological characteristics

The clinicopathological characteristics of all 231 patients included in our study are listed in Table 1. Among the 231 cases of GISTs, 192 exhibited the *KIT* exon 11 mutation, while 39 were characterized as wild type (23 cases), *PDGFRA* exon 18 mutation (12 cases), *KIT* exon 9 mutation (2 cases), *KIT* exon 17 mutation (1 case), or *PDGFRA* exon 14 mutation (1 case). Within the group of patients with the *KIT* exon 11 mutation, 56 individuals had exon 11 deletions involving codons 557-558.

Based on the results of the univariate analysis, gender, age, mitotic count, and risk classification did not show significant differences between the group with the *KIT* exon 11 mutation and the group with other types of gene mutations ($P > 0.05$ for all). However, a significant difference was observed in the mitotic count and risk classification between the group with *KIT* exon 11 codons 557-558 deletion and the group without deletions in codons 557-558 ($P < 0.01$).

CT features analysis

The primary analysis of the subjective CT features is presented in Table 2. In the univariate analysis, significant differences were observed in tumor shape, enhancement degree, and cystic change between the group with the *KIT* exon 11 mutation and the group with other types of gene mutations ($P < 0.05$). The CT features that showed statistical significance in the univariate analysis were included in the multivariate regression analysis. The results demonstrated that enhancement degree served as an independent predictor for the presence of the *KIT* exon 11 mutation. Moreover, notable disparities in CT features were observed between the group characterized by *KIT* exon 11 codons 557-558 deletion and the group lacking deletions in codons 557-558. Tumor size, tumor shape, margin, growth pattern, enhancement pattern, necrosis, intra-tumoral vessel presence, infiltration of adjacent mesangial fat, invasion of adjacent organs, and distant metastasis displayed significant differences between these two groups, as indicated by the univariate analysis. The multivariate regression analysis revealed that tumor size, tumor shape, and growth pattern were independent predictors for the presence of *KIT* exon 11 codons 557-558 deletion ($P < 0.05$).

Diagnostic performance of models

A set of 190 radiomic features, exhibiting ICC values exceeding 0.75 in intra- and inter-individual comparisons, was utilized for constructing the diagnostic model.

For *KIT* exon 11 mutation: Three CT features (gas, growth pattern, and density in arterial phase), three radiomic features (original_firstorder_Median, original_firstorder_InterquartileRange, and original_firstorder), and six clinic features (age, size, CD34, Ki-67, mitoses, and tissue-type) were extracted to build three models: $Model_{CT\ sign}$, $model_{CT\ sign + rad}$, and $model_{CT\ sign + rad + clinic}$. The combined model was developed using logistic regression, incorporating the model scores generated by each independent model. In the $model_{CT\ sign + rad}$, the Radscore was calculated as (4.58) × rad + (1.565) × ctsign + (-2.906). In the $model_{CT\ sign + rad + clinic}$, the Radscore was calculated as (4.364) × rad + (1.76) × ctsign + (5.207) × clinic + (-5.665). The training cohort exhibited AUC values of 0.743, 0.818, and 0.915 for the three models, while the validation cohort showed AUC values of 0.670, 0.781, and 0.811, respectively (Figure 2A and B). The corrected AUC values, obtained by subtracting the average optimism from the apparent AUC of the CE-CT and radiomics models, were 0.690 and 0.805, indicating relatively stable results. The diagnostic performance of the three models is presented in Table 3. Notable

Table 2 The computed tomography features of gastrointestinal stromal tumor patients included in this study, *n* (%)

Characteristics	*KIT* exon 11 mutation (*n* = 192)	Without *KIT* exon 11 mutation (*n* = 39)	*P* value	*KIT* exon 11 mutation with deletions involving codons 557-558 (*n* = 56)	*KIT* exon 11 mutation without deletions involving codons 557-558 (*n* = 136)	*P* value
Size (mm)	51 (11-224)	45 (10-201)	0.682	69 (31-224)	42.5 (11-188)	< 0.010
Shape						
Regular	66 (34.4)	7 (17.9)	0.044	5 (8.9)	61 (44.9)	< 0.010
Irregular	126 (65.6)	32 (82.1)		51 (91.1)	75 (55.1)	
Margin						
Well-defined	168 (87.5)	23 (84.6)	0.625	44 (78.6)	124 (91.2)	0.016
Ill-defined	24 (12.5)	6 (15.4)		12 (21.4)	12 (8.8)	
Growth pattern						
Endophytic	64 (33.3)	6 (15.4)	0.083	12 (21.4)	52 (38.2)	0.010
Exophytic	87 (45.3)	22 (56.4)		25 (44.6)	62 (45.6)	
Mixed	41 (21.4)	11 (28.2)		19 (33.9)	22 (16.2)	
Density						
Hypodensity	175 (91.1)	34 (87.2)	0.647	50 (89.3)	125 (91.9)	0.750
Isodensity	15 (7.8)	4 (10.3)		5 (8.9)	10 (7.4)	
Hyperdensity	2 (1.0)	1 (2.6)		1 (1.8)	1 (0.7)	
Pattern of enhancement						
Homogeneous	48 (25.0)	5 (12.8)	0.099	5 (8.9)	43 (31.6)	0.001
Heterogeneous	144 (75.0)	34 (87.2)		51 (91.1)	93 (68.4)	
Degree of enhancement						
Mild	71 (37.0)	11 (28.2)	0.018	20 (35.7)	51 (37.5)	0.063
Moderate	75 (39.1)	10 (25.6)		28 (50.0)	47 (34.6)	
Marked	46 (24.0)	18 (46.2)		8 (14.3)	38 (27.9)	
Necrosis	121 (63.0)	28 (71.8)	0.296	43 (76.8)	78 (57.4)	0.011
Gas	33 (17.2)	4 (10.3)	0.282	14 (25.0)	19 (14.0)	0.066
Cystic change	6 (3.1)	4 (10.3)	0.046	0 (0)	6 (4.4)	0.110
Calcification	23 (12.0)	2 (5.1)	0.209	8 (14.3)	15 (11.0)	0.528
Superficial ulceration	55 (28.6)	10 (25.6)	0.704	19 (33.9)	36 (26.5)	0.299
Intra-tumoral vessel	86 (44.8)	14 (35.9)	0.307	34 (60.7)	52 (38.2)	0.004
Adjacent mesangial fat infiltration	40 (20.8)	9 (23.1)	0.755	20 (35.7)	20 (14.7)	0.001
Adjacent organ invasion	29 (15.1)	7 (17.9)	0.655	14 (25.0)	15 (11.0)	0.014
Lymphadenopathy	14 (7.3)	3 (7.7)	0.930	6 (10.7)	8 (5.9)	0.242
Distant metastasis	4 (2.1)	2 (5.1)	0.276	3 (5.4)	1 (0.7)	0.042

disparities were noted among all paired diagnostic metrics for the three models in both the training and validation cohorts. The diagnostic accuracy of $model_{CT\ sign + rad + clinic}$ was significantly higher than that of $model_{CT\ sign}$ and $model_{CT\ sign + rad}$. DCA demonstrated that $model_{CT\ sign + rad + clinic}$ yielded the highest overall net benefit compared to $model_{CT\ sign}$ or $model_{CT\ sign + rad}$ in predicting the *KIT* exon 11 mutation in the training cohort across a wide range of threshold probabilities (Figure 2C). However, similar results were not observed in the validation set (Figure 2D).

Table 3 Predictive performance of different model for *KIT* exon 11 mutation

Models	$Model_{CT\ sign}$		$Model_{CT\ sign + rad}$		$Model_{CT\ sign + rad + clinic}$	
Cohort	Training	Validation	Training	Validation	Training	Validation
AUC	0.743	0.670	0.818	0.781	0.915	0.811
Accuracy	0.673	0.643	0.753	0.714	0.833	0.794
Sensitivity	0.815	0.672	0.667	0.690	0.938	0.830
Specificity	0.531	0.500	0.840	0.833	0.728	0.600
NPV	0.741	0.240	0.716	0.357	0.922	0.400
PPV	0.635	0.867	0.806	0.952	0.776	0.917

CT: Computed tomography; AUC: Area under the curve; NPV: Negative predictive value; PPV: Positive predictive value.

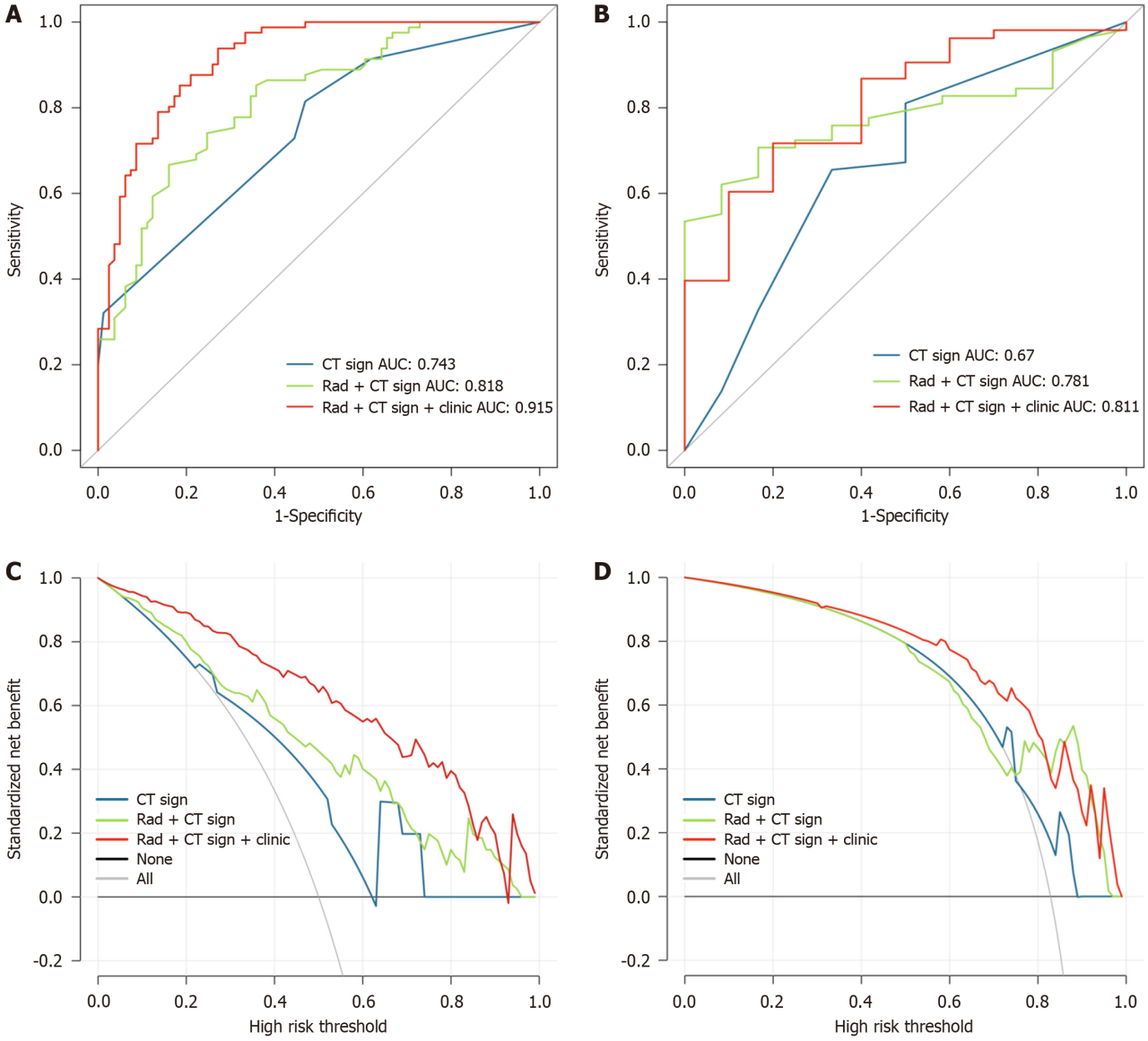

Figure 2 The discrimination ability of the radiomics model and its decision curve analysis for prediction of *KIT* exon 11 mutation. A-D: The discrimination ability of three models in the training data (A) and the validation cohort (B). The decision curve analysis for the radiomics models in the training data (C) and the validation cohort (D). AUC: Area under the curve.

For deletions in *KIT* exon 11 codons 557-558: One CT feature (shape), three radiomic features (wavelet_HLH_lbp_3D_k_firstorder_TotalEnergy, original_firstorder_Energy, and original_girlm_RunVariance), and three clinic features (Ki-67, mitoses, and tumor-size) were extracted to build three models: $Model_{CT\ sign}$, $model_{CT\ sign + rad}$, and $model_{CT\ sign + rad + clinic}$. In the $model_{CT\ sign + rad}$, the Radscore was calculated as (7.907) × rad + (4.535) × ctsign + (-3.937). In the $model_{CT\ sign + rad + clinic}$, the Radscore was calculated as (5.898) × rad + (2.636) × ctsign + (3.599) × clinic + (-4.11). The training cohort exhibited AUC values of 0.667, 0.842, and 0.872 for the three models, while the validation cohort showed AUC values of 0.61, 0.782, and 0.795, respectively (Figure 3A and B). The corrected AUC values, obtained by subtracting the average optimism from the apparent AUC of the CE-CT and radiomics models, were 0.773 and 0.751, indicating relatively stable results. The diagnostic performance of the three models is presented in Table 4. Notable variances were identified among all paired diagnostic metrics for the three models in both the training and validation cohorts. The diagnostic accuracy of $model_{CT\ sign + rad + clinic}$ was significantly higher than that of $model_{CT\ sign}$ and $model_{CT\ sign + rad}$. DCA demonstrated that $model_{CT\ sign + rad + clinic}$ produced the highest overall net benefit compared to $model_{CT\ sign}$ in predicting the deletions in *KIT* exon 11 codons 557-558 in both the training and validation cohorts across the entire risk threshold range (Figure 3A and B). However, DCA showed no significant differences between $model_{CT\ sign + rad + clinic}$ and $model_{CT\ sign + rad}$ in both the training and validation cohorts (Figure 3C and D).

DISCUSSION

Approximately 80% of GISTs harbor *KIT* mutations, while 5%-10% exhibit *PDGFRA* mutations. The presence and specific type of *KIT* and *PDGFRA* mutations are associated with the prognosis and clinical response to targeted therapy in GISTs [9,28]. Currently, mutation testing is typically performed on surgically resected tissue samples. However, some GIST patients are unable to undergo surgical resection at the time of initial diagnosis. For these patients, fine-needle biopsy samples provide adequate material for pathological examination but are insufficient for genetic analysis. Moreover, genetic testing is not routinely conducted in all hospitals due to its high cost. Therefore, there is an urgent need to establish a noninvasive, accurate, and cost-effective preoperative method for identifying the mutation status of GISTs.

CT is extensively employed in the detection, postoperative surveillance, and evaluation of treatment effectiveness in GISTs. Recent studies have identified several CT features associated with the differential diagnosis and high-risk categorization of GISTs, including tumor size, location, margin characteristics, hemorrhage, necrosis, heterogeneous enhancement, and adjacent organ invasion[29-31]. However, these conventional CT features rely on subjective analysis and the experience of radiologists, resulting in variability and lack of reproducibility. Radiomics, on the other hand, enables the extraction of high-throughput quantitative features from medical images using specific data characterization algorithms. This approach effectively reduces intra- and inter-observer variability. Importantly, radiomics has been widely applied in tumor diagnosis, prognosis prediction, and gene mutation analysis[32-36].

Several prior studies have reported the satisfactory performance of CT-based radiomics in the diagnosis and prediction of the malignant potential of GISTs[17,37-39]. Starmans *et al*[40] documented that the radiomics model achieved an AUC of 0.77 in distinguishing GISTs from non-GISTs, yielding results comparable to those of radiologists but with reduced observer dependence. Furthermore, radiomics studies in GISTs have primarily focused on predicting malignant potential and prognosis. These investigations have demonstrated the robust predictive effect and generalizability of radiomics in assessing the malignant potential of GISTs, thereby aiding clinicians in preoperative decision-making. However, there is a paucity of radiomics studies pertaining to genotype prediction. Xu *et al*[41] were the first to attempt differentiation of GISTs with and without *KIT* exon 11 mutations using CT texture analysis in a study cohort comprising 69 GISTs, with a validation group of 17 GISTs. They identified that the textural parameter standard deviation independently predicted GISTs without *KIT* exon 11 mutations, achieving AUC values of 0.726-0.750 in the study group and 0.904-0.962 in the validation group. Nonetheless, the relatively small sample sizes in this study may have impacted the accuracy of the findings. Starmans *et al*[40] also evaluated radiomics for predicting *KIT* mutational status in 123 patients with GISTs, reporting AUC values of 0.52 for *KIT* and 0.56 for *KIT* exon 11 mutation. These findings did not support the predictive value of the radiomics model in genetic features, likely due to study limitations. The remaining two studies both demonstrated the effective differentiation of GISTs with *KIT* exon 11 mutations using radiomics based on CT images[20,21]. However, the patient populations in these studies encompassed GISTs throughout the entire gastrointestinal tract, including the stomach, intestine, and colorectum, potentially introducing certain biases. It is well-known that GISTs at different sites exhibit distinct recurrence risks, with intestinal GISTs carrying a worse prognosis than gastric GISTs. Furthermore, genotypes have been closely associated with specific tumor locations, with *KIT* exon 11 mutations being most common in GISTs at all sites, while *KIT* exon 9 mutations are prevalent in intestinal GISTs, and *PDGFRA* exon 18 mutations are common in gastric GISTs[42].

Our study was derived from a large-scale imaging dataset and represents the first CT radiogenomics investigation specifically focused on gastric GISTs. The results revealed that the diagnostic accuracy of $model_{CT\ sign + rad + clinic}$ for predicting *KIT* exon 11 mutation was significantly higher than that of $model_{CT\ sign}$ and $model_{CT\ sign + rad}$, with AUC values of 0.915 in the training cohort and 0.811 in the validation cohorts. The DCA curves demonstrated that $model_{CT\ sign + rad + clinic}$ exhibited superior predictive effectiveness compared to $model_{CT\ sign}$ and $model_{CT\ sign + rad}$ in the training cohorts, highlighting the clinical benefit of the combined model in distinguishing gastric GISTs with *KIT* exon 11 mutation.

Regarding deletions in *KIT* exon 11 codons 557-558 of gastric GISTs, the diagnostic accuracy of $model_{CT\ sign + rad + clinic}$ was statistically higher than that of $model_{CT\ sign}$ and $model_{CT\ sign + rad\ model}$, with AUC values of 0.872 in the training cohort and 0.795 in the validation cohorts. The clinical benefits analysis revealed that the combined model outperformed $model_{CT\ sign}$ and $model_{CT\ sign + rad}$ in predicting the *KIT* exon 11 mutation. In the validation cohort, the sensitivity and specificity of

Table 4 Predictive performance of different model for *KIT* exon 11 codons 557-558 deletions

Models	$Model_{CT\ sign}$		$Model_{CT\ sign + rad}$		$Model_{CT\ sign + rad + clinic}$	
Cohort	Training	Validation	Training	Validation	Training	Validation
AUC	0.667	0.610	0.842	0.782	0.872	0.795
Accuracy	0.522	0.500	0.689	0.700	0.720	0.766
Sensitivity	0.949	0.824	0.974	0.824	0.923	0.667
Specificity	0.385	0.396	0.598	0.660	0.656	0.796
NPV	0.959	0.875	0.986	0.927	0.964	0.886
PPV	0.330	0.304	0.437	0.438	0.462	0.500

CT: Computed tomography; AUC: Area under the curve; NPV: Negative predictive value; PPV: Positive predictive value.

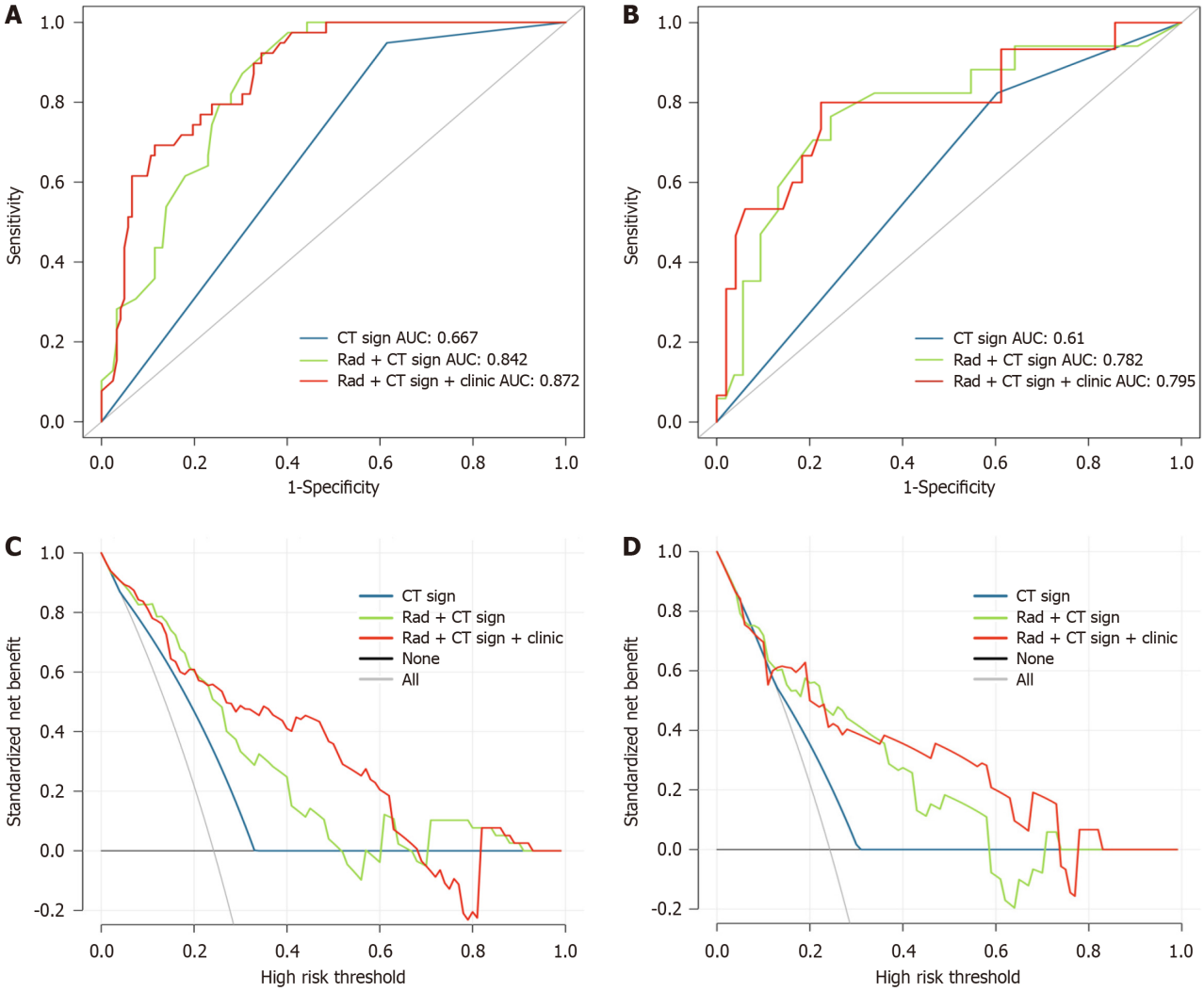

Figure 3 The discrimination ability of the radiomics model and its decision curve analysis for prediction of *KIT* exon 11 codons 557-558 deletions. A-D: The discrimination ability of three models in the training data (A) and the validation cohort (B). The decision curve analysis for the radiomics models in the training data (C) and the validation cohort (D). AUC: Area under the curve.

$model_{CT\ sign + rad + clinic}$ for predicting the *KIT* exon 11 mutation were 83.0% and 81.1%, respectively, surpassing the performance of $model_{CT\ sign}$ and $model_{CT\ sign + rad}$. The clinical benefit of the combined model was further confirmed by the DCA curves. These findings highlight the excellent predictive ability of $model_{CT\ sign + rad + clinic}$ for determining the *KIT* mutation status of gastric GISTs, suggesting its potential value in guiding noninvasive clinical decision-making prior to surgery.

However, it is important to acknowledge certain limitations in our study. Firstly, it was a retrospective study, and as such, potential selection bias could not be completely eliminated. Secondly, despite the large sample size, this study was conducted at a single center, and further validation through multicenter studies is warranted. Thirdly, due to the small sample size, we did not subdivide GISTs without *KIT* exon 11 mutation, which is crucial for clinicians to differentiate specific types of gene mutations before surgery, such as *KIT* exon 9 mutation and *PDGFRA* exon 18 mutation, as the treatment response varies.

CONCLUSION

In conclusion, our study demonstrated that the radiomics model based on CE-CT images exhibited satisfactory performance in distinguishing gastric GISTs with *KIT* exon 11 mutation and GISTs with *KIT* exon 11 codons 557-558 deletions. The combined model$_{\text{CT sign + rad + clinic}}$ demonstrated the highest predictive value, offering a potentially valuable and noninvasive approach to guide personalized treatment decisions prior to surgery.

ARTICLE HIGHLIGHTS

Research background

The assessment of *KIT* and *PDGFRA* mutations plays a vital role in establishing the pathological diagnosis of gastrointestinal stromal tumors (GISTs), predicting tumor prognosis, and guiding the administration of tyrosine kinase inhibitor therapy. For patients who are ineligible for genetic analysis, possessing information regarding the mutational status of GISTs is of paramount importance for the purpose of customizing personalized precision therapy.

Research motivation

Currently, tumor mutation status can only be obtained after surgical resection or conventional invasive biopsy, making preoperative genotyping of GISTs more challenging.

Research objectives

To develop and validate a radiomic model to predict the genotypes of gastric GISTs using contrast-enhanced computed tomography (CE-CT) images.

Research methods

The models for predicting GISTs with *KIT* exon 11 mutations or *KIT* exon 11 codons 557-558 deletions were constructed using selected clinical features, conventional CT features, and radiomics features extracted from abdominal CE-CT images. Three models were developed: Model$_{\text{CT sign}}$, model$_{\text{CT sign + rad}}$, and model$_{\text{CT sign + rad + clinic}}$. The diagnostic performance of these models was evaluated using receiver operating characteristic (ROC) curve analysis and the Delong test.

Research results

The ROC analyses demonstrated the performance of different models in predicting *KIT* exon 11 mutation and *KIT* exon 11 codons 557-558 deletions. In the training cohort, the models$_{\text{CT sign,}}$ model$_{\text{CT sign + rad}}$, and model$_{\text{CT sign + rad + clinic}}$ achieved area under the curve (AUC) values of 0.743, 0.818, and 0.915, respectively, for predicting *KIT* exon 11 mutation. In the validation cohort, the corresponding AUC values were 0.670, 0.781, and 0.811. For predicting *KIT* exon 11 codons 557-558 deletions, the AUC values in the training cohort were 0.667, 0.842, and 0.72 for model$_{\text{CT sign}}$, model$_{\text{CT sign + rad}}$, and model$_{\text{CT sign + rad + clinic}}$, respectively. In the validation cohort, the AUC values for the same models were 0.610, 0.782, and 0.795. Furthermore, the decision curve analysis confirmed the clinical significance and utility of the CT sign + rad + clinic model.

Research conclusions

Our study demonstrated that the radiomics model based on CE-CT images exhibited satisfactory performance in distinguishing gastric GISTs with *KIT* exon 11 mutation and GISTs with *KIT* exon 11 codons 557-558 deletions.

Research perspectives

This study focuses specifically on gastric GISTs and aims to develop a prediction model for genotypes using CE-CT images.

FOOTNOTES

Co-first authors: Xiao-Nan Yin and Zi-Hao Wang.

Author contributions: Yin XN and Wang ZH equally contributed to this article; Yin XN, Wang ZH, Zou L, Yang CW, Shen CY, Liu BK, Yin Y, Liu XJ, and Zhang B participated in all stages of manuscript preparation, and read and approved the final version prior to

submission.

Supported by the National Natural Science Foundation of China Program Grant, No. 82203108; China Postdoctoral Science Foundation, No. 2022M722275; Beijing Bethune Charitable Foundation, No. WCJZL202105; and Beijing Xisike Clinical Oncology Research Foundation, No. Y-zai2021/zd-0185.

Institutional review board statement: The study was reviewed and approved by the Research Ethics Board of West China Hospital, Sichuan University [approval No. 2022(449)].

Informed consent statement: The informed consent was waived by the Research Ethics Board of West China Hospital, Sichuan University.

Conflict-of-interest statement: The authors have declared that no competing interests exist.

Data sharing statement: All data analyzed during this study are included in this published article.

STROBE statement: The authors have read the STROBE Statement—checklist of items, and the manuscript was prepared and revised according to the STROBE Statement—checklist of items.

Country/Territory of origin: China

ORCID number: Xiao-Nan Yin 0000-0003-4525-1877; Cai-Wei Yang 0000-0003-3335-3948; Chao-Yong Shen 0000-0002-8426-3611; Xi-Jiao Liu 0000-0002-6900-0696; Bo Zhang 0000-0002-0254-5843.

S-Editor: Chen YL
L-Editor: A
P-Editor: Zheng XM

REFERENCES

1 **Blay JY**, Kang YK, Nishida T, von Mehren M. Gastrointestinal stromal tumours. *Nat Rev Dis Primers* 2021; **7**: 22 [PMID: 33737510 DOI: 10.1038/s41572-021-00254-5]
2 **Søreide K**, Sandvik OM, Søreide JA, Giljaca V, Jureckova A, Bulusu VR. Global epidemiology of gastrointestinal stromal tumours (GIST): A systematic review of population-based cohort studies. *Cancer Epidemiol* 2016; **40**: 39-46 [PMID: 26618334 DOI: 10.1016/j.canep.2015.10.031]
3 **Corless CL**, Barnett CM, Heinrich MC. Gastrointestinal stromal tumours: origin and molecular oncology. *Nat Rev Cancer* 2011; **11**: 865-878 [PMID: 22089421 DOI: 10.1038/nrc3143]
4 **Klug LR**, Khosroyani HM, Kent JD, Heinrich MC. New treatment strategies for advanced-stage gastrointestinal stromal tumours. *Nat Rev Clin Oncol* 2022; **19**: 328-341 [PMID: 35217782 DOI: 10.1038/s41571-022-00606-4]
5 **Pierotti MA**, Tamborini E, Negri T, Pricl S, Pilotti S. Targeted therapy in GIST: in silico modeling for prediction of resistance. *Nat Rev Clin Oncol* 2011; **8**: 161-170 [PMID: 21364689 DOI: 10.1038/nrclinonc.2011.3]
6 **Dermawan JK**, Rubin BP. Molecular Pathogenesis of Gastrointestinal Stromal Tumor: A Paradigm for Personalized Medicine. *Annu Rev Pathol* 2022; **17**: 323-344 [PMID: 34736340 DOI: 10.1146/annurev-pathol-042220-021510]
7 **Boikos SA**, Pappo AS, Killian JK, LaQuaglia MP, Weldon CB, George S, Trent JC, von Mehren M, Wright JA, Schiffman JD, Raygada M, Pacak K, Meltzer PS, Miettinen MM, Stratakis C, Janeway KA, Helman LJ. Molecular Subtypes of KIT/PDGFRA Wild-Type Gastrointestinal Stromal Tumors: A Report From the National Institutes of Health Gastrointestinal Stromal Tumor Clinic. *JAMA Oncol* 2016; **2**: 922-928 [PMID: 27011036 DOI: 10.1001/jamaoncol.2016.0256]
8 **Corless CL**, Schroeder A, Griffith D, Town A, McGreevey L, Harrell P, Shiraga S, Bainbridge T, Morich J, Heinrich MC. PDGFRA mutations in gastrointestinal stromal tumors: frequency, spectrum and in vitro sensitivity to imatinib. *J Clin Oncol* 2005; **23**: 5357-5364 [PMID: 15928335 DOI: 10.1200/jco.2005.14.068]
9 **Rossi S**, Gasparotto D, Miceli R, Toffolatti L, Gallina G, Scaramel E, Marzotto A, Boscato E, Messerini L, Bearzi I, Mazzoleni G, Capella C, Arrigoni G, Sonzogni A, Sidoni A, Mariani L, Amore P, Gronchi A, Casali PG, Maestro R, Dei Tos AP. KIT, PDGFRA, and BRAF mutational spectrum impacts on the natural history of imatinib-naive localized GIST: a population-based study. *Am J Surg Pathol* 2015; **39**: 922-930 [PMID: 25970686 DOI: 10.1097/PAS.0000000000000418]
10 **Joensuu H**. Risk stratification of patients diagnosed with gastrointestinal stromal tumor. *Hum Pathol* 2008; **39**: 1411-1419 [PMID: 18774375 DOI: 10.1016/j.humpath.2008.06.025]
11 **Joensuu H**, Rutkowski P, Nishida T, Steigen SE, Brabec P, Plank L, Nilsson B, Braconi C, Bordoni A, Magnusson MK, Sufliarsky J, Federico M, Jonasson JG, Hostein I, Bringuier PP, Emile JF. KIT and PDGFRA mutations and the risk of GI stromal tumor recurrence. *J Clin Oncol* 2015; **33**: 634-642 [PMID: 25605837 DOI: 10.1200/JCO.2014.57.4970]
12 **Hong JH**, Jung JY, Jo A, Nam Y, Pak S, Lee SY, Park H, Lee SE, Kim S. Development and Validation of a Radiomics Model for Differentiating Bone Islands and Osteoblastic Bone Metastases at Abdominal CT. *Radiology* 2021; **299**: 626-632 [PMID: 33787335 DOI: 10.1148/radiol.2021203783]

13 **Kirienko M**, Sollini M, Corbetta M, Voulaz E, Gozzi N, Interlenghi M, Gallivanone F, Castiglioni I, Asselta R, Duga S, Soldà G, Chiti A. Radiomics and gene expression profile to characterise the disease and predict outcome in patients with lung cancer. *Eur J Nucl Med Mol Imaging* 2021; **48**: 3643-3655 [PMID: 33959797 DOI: 10.1007/s00259-021-05371-7]

14 **Li L**, Kan X, Zhao Y, Liang B, Ye T, Yang L, Zheng C. Radiomics Signature: A potential biomarker for the prediction of survival in Advanced Hepatocellular Carcinoma. *Int J Med Sci* 2021; **18**: 2276-2284 [PMID: 33967603 DOI: 10.7150/ijms.55510]

15 **Schniering J**, Maciukiewicz M, Gabrys HS, Brunner M, Blüthgen C, Meier C, Braga-Lagache S, Uldry AC, Heller M, Guckenberger M, Fretheim H, Nakas CT, Hoffmann-Vold AM, Distler O, Frauenfelder T, Tanadini-Lang S, Maurer B. Computed tomography-based radiomics decodes prognostic and molecular differences in interstitial lung disease related to systemic sclerosis. *Eur Respir J* 2022; **59** [PMID: 34649979 DOI: 10.1183/13993003.04503-2020]

16 **Chen T**, Ning Z, Xu L, Feng X, Han S, Roth HR, Xiong W, Zhao X, Hu Y, Liu H, Yu J, Zhang Y, Li Y, Xu Y, Mori K, Li G. Radiomics nomogram for predicting the malignant potential of gastrointestinal stromal tumours preoperatively. *Eur Radiol* 2019; **29**: 1074-1082 [PMID: 30116959 DOI: 10.1007/s00330-018-5629-2]

17 **Chen Z**, Xu L, Zhang C, Huang C, Wang M, Feng Z, Xiong Y. CT Radiomics Model for Discriminating the Risk Stratification of Gastrointestinal Stromal Tumors: A Multi-Class Classification and Multi-Center Study. *Front Oncol* 2021; **11**: 654114 [PMID: 34168985 DOI: 10.3389/fonc.2021.654114]

18 **Wang C**, Li H, Jiaerken Y, Huang P, Sun L, Dong F, Huang Y, Dong D, Tian J, Zhang M. Building CT Radiomics-Based Models for Preoperatively Predicting Malignant Potential and Mitotic Count of Gastrointestinal Stromal Tumors. *Transl Oncol* 2019; **12**: 1229-1236 [PMID: 31280094 DOI: 10.1016/j.tranon.2019.06.005]

19 **Zhao Y**, Feng M, Wang M, Zhang L, Li M, Huang C. CT Radiomics for the Preoperative Prediction of Ki67 Index in Gastrointestinal Stromal Tumors: A Multi-Center Study. *Front Oncol* 2021; **11**: 689136 [PMID: 34595107 DOI: 10.3389/fonc.2021.689136]

20 **Liu B**, Liu H, Zhang L, Song Y, Yang S, Zheng Z, Zhao J, Hou F, Zhang J. Value of contrast-enhanced CT based radiomic machine learning algorithm in differentiating gastrointestinal stromal tumors with KIT exon 11 mutation: a two-center study. *Diagn Interv Radiol* 2022; **28**: 29-38 [PMID: 35142612 DOI: 10.5152/dir.2021.21600]

21 **Liu X**, Yin Y, Wang X, Yang C, Wan S, Yin X, Wu T, Chen H, Xu Z, Li X, Song B, Zhang B. Gastrointestinal stromal tumors: associations between contrast-enhanced CT images and KIT exon 11 gene mutation. *Ann Transl Med* 2021; **9**: 1496 [PMID: 34805358 DOI: 10.21037/atm-21-3811]

22 **Palatresi D**, Fedeli F, Danti G, Pasqualini E, Castiglione F, Messerini L, Massi D, Bettarini S, Tortoli P, Busoni S, Pradella S, Miele V. Correlation of CT radiomic features for GISTs with pathological classification and molecular subtypes: preliminary and monocentric experience. *Radiol Med* 2022; **127**: 117-128 [PMID: 35022956 DOI: 10.1007/s11547-021-01446-5]

23 **van Griethuysen JJM**, Fedorov A, Parmar C, Hosny A, Aucoin N, Narayan V, Beets-Tan RGH, Fillion-Robin JC, Pieper S, Aerts HJWL. Computational Radiomics System to Decode the Radiographic Phenotype. *Cancer Res* 2017; **77**: e104-e107 [PMID: 29092951 DOI: 10.1158/0008-5472.CAN-17-0339]

24 **Chawla NV**, Bowyer KW, Hall LO, Kegelmeyer WP. Smote: Synthetic minority over-sampling technique. *J AI Res* 2002; **16**: 321-357 [DOI: 10.48550/arXiv.1106.1813]

25 **Breiman L**. Random Forests. *Machine Learning* 2001; **45**: 5-32 [DOI: 10.1023/A:1010933404324]

26 **Rokach L**. Decision Forest: Twenty years of research. *Information Fusion* 2016; **27**: 111-125 [DOI: 10.1016/j.inffus.2015.06.005]

27 **Steyerberg EW**, Harrell FE Jr, Borsboom GJ, Eijkemans MJ, Vergouwe Y, Habbema JD. Internal validation of predictive models: efficiency of some procedures for logistic regression analysis. *J Clin Epidemiol* 2001; **54**: 774-781 [PMID: 11470385 DOI: 10.1016/s0895-4356(01)00341-9]

28 **Heinrich MC**, Maki RG, Corless CL, Antonescu CR, Harlow A, Griffith D, Town A, McKinley A, Ou WB, Fletcher JA, Fletcher CD, Huang X, Cohen DP, Baum CM, Demetri GD. Primary and secondary kinase genotypes correlate with the biological and clinical activity of sunitinib in imatinib-resistant gastrointestinal stromal tumor. *J Clin Oncol* 2008; **26**: 5352-5359 [PMID: 18955458 DOI: 10.1200/JCO.2007.15.7461]

29 **Chen Z**, Yang J, Sun J, Wang P. Gastric gastrointestinal stromal tumours (2-5 cm): Correlation of CT features with malignancy and differential diagnosis. *Eur J Radiol* 2020; **123**: 108783 [PMID: 31841880 DOI: 10.1016/j.ejrad.2019.108783]

30 **Xu JX**, Ding QL, Lu YF, Fan SF, Rao QP, Yu RS. A scoring model for radiologic diagnosis of gastric leiomyomas (GLMs) with contrast-enhanced computed tomography (CE-CT): Differential diagnosis from gastrointestinal stromal tumors (GISTs). *Eur J Radiol* 2021; **134**: 109395 [PMID: 33310552 DOI: 10.1016/j.ejrad.2020.109395]

31 **Zhou C**, Duan X, Zhang X, Hu H, Wang D, Shen J. Predictive features of CT for risk stratifications in patients with primary gastrointestinal stromal tumour. *Eur Radiol* 2016; **26**: 3086-3093 [PMID: 26699371 DOI: 10.1007/s00330-015-4172-7]

32 **Balana C**, Castañer S, Carrato C, Moran T, Lopez-Paradís A, Domenech M, Hernandez A, Puig J. Preoperative Diagnosis and Molecular Characterization of Gliomas With Liquid Biopsy and Radiogenomics. *Front Neurol* 2022; **13**: 865171 [PMID: 35693015 DOI: 10.3389/fneur.2022.865171]

33 **Harding-Theobald E**, Louissaint J, Maraj B, Cuaresma E, Townsend W, Mendiratta-Lala M, Singal AG, Su GL, Lok AS, Parikh ND. Systematic review: radiomics for the diagnosis and prognosis of hepatocellular carcinoma. *Aliment Pharmacol Ther* 2021; **54**: 890-901 [PMID: 34390014 DOI: 10.1111/apt.16563]

34 **Lu J**, Li X, Li H. A radiomics feature-based nomogram to predict telomerase reverse transcriptase promoter mutation status and the prognosis of lower-grade gliomas. *Clin Radiol* 2022; **77**: e560-e567 [PMID: 35595562 DOI: 10.1016/j.crad.2022.04.005]

35 **Sohn B**, An C, Kim D, Ahn SS, Han K, Kim SH, Kang SG, Chang JH, Lee SK. Radiomics-based prediction of multiple gene alteration incorporating mutual genetic information in glioblastoma and grade 4 astrocytoma, IDH-mutant. *J Neurooncol* 2021; **155**: 267-276 [PMID: 34648115 DOI: 10.1007/s11060-021-03870-z]

36 **Staal FCR**, van der Reijd DJ, Taghavi M, Lambregts DMJ, Beets-Tan RGH, Maas M. Radiomics for the Prediction of Treatment Outcome and Survival in Patients With Colorectal Cancer: A Systematic Review. *Clin Colorectal Cancer* 2021; **20**: 52-71 [PMID: 33349519 DOI: 10.1016/j.clcc.2020.11.001]

37 **Shao M**, Niu Z, He L, Fang Z, He J, Xie Z, Cheng G, Wang J. Building Radiomics Models Based on Triple-Phase CT Images Combining Clinical Features for Discriminating the Risk Rating in Gastrointestinal Stromal Tumors. *Front Oncol* 2021; **11**: 737302 [PMID: 34950578 DOI: 10.3389/fonc.2021.737302]

38 **Wang M**, Feng Z, Zhou L, Zhang L, Hao X, Zhai J. Computed-Tomography-Based Radiomics Model for Predicting the Malignant Potential of Gastrointestinal Stromal Tumors Preoperatively: A Multi-Classifier and Multicenter Study. *Front Oncol* 2021; **11**: 582847 [PMID: 33968714 DOI: 10.3389/fonc.2021.582847]

39 **Zhang QW**, Zhou XX, Zhang RY, Chen SL, Liu Q, Wang J, Zhang Y, Lin J, Xu JR, Gao YJ, Ge ZZ. Comparison of malignancy-prediction efficiency between contrast and non-contract CT-based radiomics features in gastrointestinal stromal tumors: A multicenter study. *Clin Transl Med* 2020; **10**: e291 [PMID: 32634272 DOI: 10.1002/ctm2.91]

40 **Starmans MPA**, Timbergen MJM, Vos M, Renckens M, Grünhagen DJ, van Leenders GJLH, Dwarkasing RS, Willemssen FEJA, Niessen WJ, Verhoef C, Sleijfer S, Visser JJ, Klein S. Differential Diagnosis and Molecular Stratification of Gastrointestinal Stromal Tumors on CT Images Using a Radiomics Approach. *J Digit Imaging* 2022; **35**: 127-136 [PMID: 35088185 DOI: 10.1007/s10278-022-00590-2]

41 **Xu F**, Ma X, Wang Y, Tian Y, Tang W, Wang M, Wei R, Zhao X. CT texture analysis can be a potential tool to differentiate gastrointestinal stromal tumors without KIT exon 11 mutation. *Eur J Radiol* 2018; **107**: 90-97 [PMID: 30292279 DOI: 10.1016/j.ejrad.2018.07.025]

42 **Lasota J**, Miettinen M. Clinical significance of oncogenic KIT and PDGFRA mutations in gastrointestinal stromal tumours. *Histopathology* 2008; **53**: 245-266 [PMID: 18312355 DOI: 10.1111/j.1365-2559.2008.02977.x]

Published by **Baishideng Publishing Group Inc**
7041 Koll Center Parkway, Suite 160, Pleasanton, CA 94566, USA
Telephone: +1-925-3991568
E-mail: office@baishideng.com
Help Desk: https://www.f6publishing.com/helpdesk
https://www.wjgnet.com